Slow-wave amplifiers and oscillators: A unified study

Levi Schächter and John A. Nation
Laboratory of Plasma Studies, Cornell University, Ithaca, New York 14853
and School of Electrical Engineering, Cornell University, Ithaca, New York 14853

(Received 30 August 1991)

In an idealized model of a traveling-wave amplifier operating in the linear regime it is assumed that all the transients have decayed. This implies that the electromagnetic wave has an amplitude which is constant in time but may vary in space according to the interaction process. In an idealized model of an oscillator, the situation is reversed. The amplitude of the electromagnetic wave is constant in space and it may vary in time. We present a generalized formulation of the interaction in a traveling-wave tube which includes reflections and spatial and temporal transients. Within this framework it is shown that, in an amplifier, the reflections cause time variations of the amplitude that are ultimately revealed as a broadening of the spectrum. The "transition" to an oscillator is also investigated. In the case of an oscillator, it is shown that in addition to the well-known temporal transient (lethargy) there is a spatial transient. This is due to the fact that it takes part of the system length for the "fresh" electrons entering the oscillator to get bunched. Beyond this transient the amplitude is constant in space, as anticipated by the idealized theory.

PACS number(s): 41.60.Cr, 52.75.Ms, 41.75.Fr

I. INTRODUCTION

A significant amount of experimental and theoretical effort [1–17] has been directed toward generation of microwave power using slow-wave structures. The devices under investigation fall in two categories: amplifiers or oscillators. Each of these categories can be divided in two subcategories corresponding to the way the phase velocity is slowed down: periodic boundary condition or dielectrically loaded waveguide. In the first case, a very large number of spatial (Floquet) harmonics are excited for a given frequency; each harmonic having a different phase velocity. The system is designed so that the harmonic which is synchronous with the electrons is dominant. In the other case, a waveguide is partially filled with dielectric material and, if properly designed, only a single wave may propagate through. There are advantages and disadvantages to both systems but the interaction process is always the same.

The energy exchange is between an ensemble of electrons and an electromagnetic wave which has a phase velocity that is relatively close to the average velocity of the particles. A strong magnetic field guides the electrons so that their motion is mainly longitudinal. As a result, it is the z component of the electric field (TM_{01} mode) which is practically the only one which participates in the interaction process. Moreover, only the wave which is propagating parallel to the electrons is interacting. The power flow can be either parallel to the beam if the phase and the group velocity have the same sign or antiparallel otherwise, the system being referred to as a forward-wave or backward-wave device, respectively. Although only the propagating wave interacts with the electrons, a backward wave always coexists in the structure because of the impedance mismatch at both ends. This wave provides the positive feedback necessary for the operation of the system as an oscillator or can be destructive in an amplifier. Experimental results in the past three years have led to a theoretical study to understand the effect of reflections in an amplifier. The outcome of this effort so far has been (i) to show that the product gain bandwidth in an amplifier is constant and it equals the bandwidth of the amplifier when no electrons are injected [12]. (ii) Asymmetric sidebands may occur in an amplifier due to amplified noise at frequencies selected by the constructive interference of the two counterpropagating waves [16]. (iii) It is possible to tune an amplifier in a narrow range of frequencies by introducing a "quarter-wavelength cavity" in the interaction region [17]. One of the main conclusions of this effort was that the convenient picture that a system may operate either as an amplifier or as an oscillator is too simplistic and any device operates somewhere in between these two regimes.

Let us first explain what we mean by the simplistic models of an amplifier or oscillator. As a linear device, an amplifier should be designed to operate in such a way that the time variation of the output signal is determined only by the generator at the input. For this purpose three conditions have to be satisfied: (1) the reflected wave has to be negligible, (2) the electron pulse is very long (on the time scale we wish the system to be linear), and (3) the system does not reach saturation. Within the framework of this idealized picture what remains to be established is the space variation along the interaction region. In other words, the amplitude of the electromagnetic wave is an amplifier is *constant in time but it varies in space* according to the interaction process.

If zero reflection is one of the conditions for no variations in time of the amplitude in an amplifier, it is exactly the opposite case for an oscillator. In fact the latter is designed with two "short circuiting" planes that confine most of the electromagnetic energy; in addition there is no external generator. These (idealized) planes impose some boundary conditions which practically enforce the spatial variation of the electromagnetic wave. As electrons are injected, the problem is to determine the time variation of the electromagnetic waves and the electrons. Within this idealized framework it is assumed that the amplitude of the electromagnetic wave in an oscillator is *constant in space but it varies in time* according to the interaction process.

In practice we always have some reflected wave in an amplifier and therefore the amplitude cannot be constant in time whereas in an oscillator, it is expected to have some variation in space. The goal of this study is to investigate these deviations from the idealized models of an amplifier or an oscillator.

For this purpose the equations which describe the dynamics of an amplifier and an oscillator are formulated in a general form. It is shown that subject to the assumptions mentioned previously, this general set of equations simplifies to the set of equations which describe an ideal amplifier or oscillator, corresponding to the conditions of operation. Solutions of the idealized models will be presented. Based on these solutions, it is shown that reflections may cause a variation in time of the amplitude of the interacting wave in an amplifier. This immediately implies that the spectrum of the amplified wave is broadened, a phenomenon observed experimentally. The effect of the reflections on the broadening is presented. Considering a particular system, we show how the regime of operation depends on the reflection coefficients at both ends. For simplicity it is assumed that both coefficients are equal, ρ. If $|\rho|$ is small then the amplitude is indeed constant in time and the system is operating as an idealized amplifier. Increasing the value of ρ, the system saturates and the amplitude varies in space and in time. A further increase of the reflection coefficient causes a zero spatial gain and all the gain is due to *variation in time* of the amplitude. In an oscillator, the variation in space of the amplitude results from two different processes: the first is the energy loss through the reflecting planes and the second is the finite length it takes the radiation field to bunch the fresh electrons entering the system.

The article is arranged as follows: in the next section we develop the general set of equations that describe the dynamics of an amplifier and an oscillator. In Sec. III the idealized models of an amplifier and an oscillator are presented. Afterward, the amplifier is examined with special emphasis on the effect of the reflections on the gain and spectrum of the output signal. In Sec. V we analyze the interaction in an oscillator.

II. DYNAMICS OF THE SYSTEM

A. General

The presence of the strong guiding magnetic field allows only transverse magnetic (TM) modes to interact with the beam. In the present analysis we shall limit the discussion to a single mode, namely, the TM_{01}. The electromagnetic field in this case can be derived from the z component of the magnetic vector potential that is a solution of

$$\left[\nabla^2-\frac{1}{c^2}\frac{\partial^2}{\partial t^2}\right]A_z(r,z,t)=-\mu_0 J_z(r,z,t) \; . \tag{2.1}$$

The current density $J_z(r,z,t)$ has an azimuthal symmetry and is determined by the motion of the electrons through

$$J_z(r,z,t)=-e\sum_i V_{z,i}(t)\delta[r-r_i(t)]\frac{1}{2\pi r}\delta[z-z_i(t)] \; . \tag{2.2}$$

Since all the motion is longitudinal, $r_i(t)=r_i(0)$, the dynamics of the electrons is a solution of

$$mc^2\frac{d\gamma_i(t)}{dt}=-eV_{z,i}(t)E_z[r=r_i(t),z=z_i(t),t] \; , \tag{2.3}$$

which represents the one-particle energy conservation. In these equations $V_{z,i}$ denotes the ith electron velocity and $\gamma_i\equiv 1/[1-(V_{z,i}/c)^2]^{1/2}$. For a solution of this set of equations one should know the initial conditions of all the particles, fields, and the boundary conditions imposed on the electromagnetic field. The relation between the magnetic vector potential and all the components of the radiation field is given by

$$E_r(r,z,t)=c^2\int dt\frac{\partial^2}{\partial r\partial z}A_z(r,z,t) \; , \tag{2.4}$$

$$E_z(r,z,t)=c^2\int dt\left[-\frac{1}{c^2}\frac{\partial^2}{\partial t^2}+\frac{\partial t^2}{\partial z^2}\right]A_z(r,z,t) \; , \tag{2.5}$$

$$H_\theta(r,z,t)=-\frac{1}{\mu_0}\frac{\partial A_z(R,z,t)}{\partial r} \; . \tag{2.6}$$

Based on this set of equations [Eqs. (2.1)–(2.6)] we shall determine a set of simplified equations to describe the interaction between electrons and waves in a slow-wave structure operating either as an amplifier or as an oscillator.

B. Global energy conservation

Typically the wave present in the system is oscillating with an angular frequency ω which is significantly faster than all other variations. Furthermore, the spatial variation is also oscillatory with a wave number k, in other words, the magnetic vector potential is assumed to have the form

$$\begin{aligned}A_z(r,z,t)=&A_+(r,z,t)\cos[\omega t-kz-\psi_+(z,t)]\\&+A_-(r,z,t)\cos[\omega t+kz-\psi_-(z,t)] \; ,\end{aligned} \tag{2.7}$$

where the variation of the amplitudes and phases on z and t is assumed to be much slower than that of the trigonometric function. Based on this assumption we may write the Poynting theorem

$$\nabla\cdot\mathbf{S}(r,z,t)+\frac{\partial}{\partial t}W_{\rm em}(r,z,t)=-J_z(r,z,t)E_z(r,z,t) \; , \tag{2.8}$$

in an integral form

$$\frac{\partial}{\partial z}[P_+(z,t)-P_-(z,t)]+\frac{\partial}{\partial t}[W_+(z,t)+W_-(z,t)] = -mc^2\sum_i \delta[z-z_i(t)]\frac{d\gamma_i(t)}{dt} , \quad (2.9)$$

where we have ignored terms oscillating at twice the wave frequency and substituted for J_z and E_z from Eqs. (2.2) and (2.3). The power and the energy associated with these two waves may be expressed in the form

$$P_\pm(z,t)=\frac{c^2k}{2\mu_0\omega}2\pi\int_\sigma dr\, r\left[\frac{\partial A_\pm(r,z,t)}{\partial r}\right]^2 \quad (2.10)$$

and

$$W_\pm(z,t)=\frac{1}{4\mu_0}2\pi\int_\sigma dr\, r\left[\frac{\partial A_\pm(r,z,t)}{\partial r}\right]^2\left[1+\left[\frac{kc}{\omega}\right]^2\right]+\frac{1}{4\mu_0}2\pi\int_\sigma dr\, r\left\{A_\pm(r,z,t)\frac{\omega}{c}\left[1-\left[\frac{kc}{\omega}\right]^2\right]\right\}^2 , \quad (2.11)$$

where σ denotes the system's cross section. It is interesting to note that using the macroscopic charge conservation law, one can immediately write Eq. (2.9) in a form of a conservation law, namely,

$$\frac{\partial}{\partial z}\left[P_+(z,t)-P_-(z,t)+mc^2\sum_i\delta[z-z_i(t)]V_{z,i}(t)[\gamma_i(t)-1]\right] + \frac{\partial}{\partial t}\left[W_+(z,t)+W_-(z,t)+mc^2\sum_i\delta[z-z_i(t)][\gamma_i(t)-1]\right]=0 , \quad (2.12)$$

where in the first term we can identify the kinetic energy flux, whereas in the second, the last expression is the total kinetic energy associated with the motion of the electrons.

From the initial expression for the Poynting theorem we can write

$$\frac{\partial}{\partial z}[P_+(z,t)-P_-(z,t)]+\frac{\partial}{\partial t}[W_+(z,t)+W_-(z,t)] = e\tfrac{1}{2}[E_+(z,t)N\langle\delta[z-z_i(t)]V_{z,i}e^{j\chi_i}\rangle+\text{c.c.}] , \quad (2.13)$$

where $E_+(z,t)$ is the z component of the electric field *at the electron's location* ($r=r_e$), i.e.,

$$E_+(z,t)=\frac{c^2}{j\omega}\left[\frac{\omega^2}{c^2}-k^2\right]A_+(r=r_e,z,t)e^{-j\psi_+(z,t)} . \quad (2.14)$$

It is tacitly assumed here that the beam thickness is small on the scale of the wavelength and the electric field is uniform across its cross section. The notation $\langle\ \rangle$ indicates averaging over the entire ensemble of N electrons present in the interaction region. The phase between the wave and the particle is denoted by χ_i and it is given by

$$\chi_i(t)\equiv\omega t-kz_i(t) . \quad (2.15)$$

Next we write the power flowing in the system in terms of the amplitude of the electric field at the electrons' location. Denoting the cross-section surface by s, we can write the total average power flowing forward in terms of the amplitude of the electric field (E_+) affecting the electrons as

$$P_+(z,t)=\frac{s}{2Z_{\text{eff}}}|E_+(z,t)|^2 ; \quad (2.16)$$

in a similar way, we may write the total electromagnetic energy stored in the forward wave

$$W_+(z,t)=\frac{s}{2}\epsilon_0\epsilon_{\text{eff}}|E_+(z,t)|^2 . \quad (2.17)$$

Similar expressions can be written for the backward wave; both the effective impedance Z_{eff} and the effective "dielectric" coefficient ϵ_{eff} remain the same. These two quantities depend on the cold characteristics of the structure and on the location of the beam in the guide; Eqs. (2.16) and (2.17) should be regarded as their definitions.

C. Simplified equations

With these definitions in mind we may now reformulate the equations which describe the dynamics of the wave and the electrons in the interaction region. Denoting by $a_\pm\equiv eE_\pm d/mc^2$ the normalized amplitude of the z component of the electric field in the vicinity of the electrons, $\bar z=z/d$, $\tau=tc/d$ where d is the total length of the system, we may write the one-particle energy conservation [Eq. (2.3)] as

$$\frac{d}{d\tau}\gamma_i(\tau)=-\beta_i\tfrac{1}{2}[a_+(\bar z=\bar z_i(\tau),\tau)e^{j\chi_i(\tau)}+\text{c.c.}] , \quad (2.18)$$

whereas the global energy conservation yields

$$\frac{\partial}{\partial\tau}[|a_+(\bar z,\tau)|^2+|a_-(\bar z,\tau)|^2]+\beta_E\frac{\partial}{\partial\bar z}[|a_+(\bar z,\tau)|^2-|a_-(\bar z,\tau)|^2]=\alpha[a_+(\bar z,\tau)\langle\delta[\bar z-\bar z_i(\tau)]\beta_i e^{j\chi_i(\tau)}\rangle+\text{c.c.}] . \quad (2.19)$$

The coupling coefficient α is defined as

$$\alpha \equiv \frac{eI(\mu_0/\epsilon_0)^{1/2}}{mc^2} \frac{1}{\epsilon_{\text{eff}}} \frac{d^2}{s} \frac{1}{\langle \beta \rangle_0} , \tag{2.20}$$

$\langle \beta \rangle_0$ is the average (normalized) velocity of the electrons at the input. The normalized energy velocity β_E is given by

$$\beta_E \equiv \frac{(\mu_0/\epsilon_0)^{1/2}}{Z_{\text{eff}}\epsilon_{\text{eff}}} , \tag{2.21}$$

and it is independent of the beam location. The relation between the amplitude of the forward wave $[a_+(\bar{z},\tau)]$ and that of the backward wave $[a_-(\bar{z},\tau)]$, in the presence of the beam, is determined by the reflection coefficients and the initial amplitude of the forward propagating wave in the absence of the electron beam, which we shall denote by a_0. At any instant τ, the *change* in the forward-wave amplitude is reflected from the output end towards the input according to

$$[a_+(1,\tau)-a_0]\rho_{\text{out}}e^{-jkd} . \tag{2.22}$$

The backward wave is not directly affected by the beam and therefore propagates towards the input with the wave energy velocity, and after a delay, $1/\beta_E$, it undergoes an additional reflection. The contribution of the reflection at the input is given by

$$a_+(0,\tau)-a_0=R[a_+(1,\tau-1/\beta_E)-a_0] , \tag{2.23}$$

where $R\equiv\rho_{\text{in}}\rho_{\text{out}}e^{-2jkd}$ is the total reflection [18] and phase shift the wave undergoes during its round trip. This is the condition imposed by the reflections on the amplitude of the interacting wave.

Since the backward wave propagates unaffected by the beam, its amplitude satisfies

$$\left[\frac{\partial}{\partial\tau}-\beta_E\frac{\partial}{\partial\bar{z}}\right]|a_-(\bar{z},\tau)|^2=0 . \tag{2.24}$$

Substituting the last relation in the expression for the global energy conservation [Eq. (2.19)] and assuming that $a_+(\bar{z},\tau)$ is not identically zero, we can simplify Eq. (2.19) to read

$$\left[\frac{\partial}{\partial\tau}+\beta_E\frac{\partial}{\partial\bar{z}}\right]a_+(\bar{z},\tau)=\alpha\langle\delta[\bar{z}-\bar{z}_i(\tau)]\beta_i e^{-j\chi_i(\tau)}\rangle . \tag{2.25}$$

Equations (2.18), (2.23), and (2.25) are the set of equations that describe the interaction between electrons and the radiation field in a slow-wave structure. Examining these equations it is clearly revealed by Eq. (2.23) that the reflections relate the amplitude of the radiation field at a given time at the input with the amplitude at the output at an earlier time, causing, therefore, time variations. For a solution of this set of equations, one ought to know the initial conditions, i.e., the location and the velocity of the electrons at $\tau=0$ as well as the radiation field.

III. IDEALIZED MODEL

A. Amplifier

Within the framework of the idealized amplifier, we may neglect reflections and no variations in time of the amplitude occur. Both the electrons' energy and the field amplitude are varying in space. At a point $\bar{z}$ along the amplifier, the energy of the electrons is varying according to

$$\frac{d}{d\bar{z}}\gamma_i(\bar{z})=-\tfrac{1}{2}[a_+(\bar{z})e^{j\chi(\bar{z})}+\text{c.c.}] . \tag{3.1}$$

The phase is conveniently redefined to read

$$\chi_i(\bar{z})=\chi_i(0)+\int_0^{\bar{z}}d\xi\left[\frac{\Omega}{\beta_i(\xi)}-K\right] , \tag{3.2}$$

where $\Omega\equiv\omega d/c$, $K\equiv kd$, and $\int_0^{\bar{z}}d\xi/\beta_i(\xi)$ is the normalized time it takes the ith particle to reach the point $\bar{z}$ starting from $\bar{z}=0$. In order to establish the equation for the amplitude of the electromagnetic field we average Eq. (2.25) over a period of time τ_0 which corresponds to the average time it takes an electron to cross the amplifier, i.e.,

$$\tau_0\equiv\int_0^1 d\xi\left\langle\frac{1}{\beta_i(\xi)}\right\rangle . \tag{3.3}$$

Assuming that none of the electrons is reflected back to the input in the interaction process, i.e., β_i is not zero for any i and any $\bar{z}$, we may write

$$\frac{d}{d\bar{z}}a_+(\bar{z})=\frac{\alpha}{\tau_0\beta_E}\langle e^{-j\chi_i(\bar{z})}\rangle , \tag{3.4}$$

in which we have tacitly assumed that in the period of time τ_0 no variation in the amplitude occurs. Equations (3.1), (3.2), and (3.4) are the equations that describe the dynamics of the fields and the particles in an idealized amplifier. Since the reflections are assumed to be zero Eq. (2.23) is trivial since $a_+(0,\tau)=a_0$ and $R=0$.

Within the framework of this formulation, the well-known gain expression as established by Pierce can be determined as follows. We calculate the third derivative of $a_+(\bar{z})$ using these two equations. Neglecting rapidly oscillating terms we find

$$\left[\frac{d^3}{d\bar{z}^3}-j\frac{\alpha\Omega}{2\tau_0\beta_E}\left\langle\frac{1}{(\gamma_i\beta_i)^3}\right\rangle\right]a_+(\bar{z}) =\frac{\alpha K}{\tau_0\beta_E}\left\langle\left[\frac{\Omega}{\beta_i}-K\right]e^{-j\chi_i}\right\rangle . \tag{3.5}$$

Assuming that $\langle 1/(\gamma_i\beta_i)^3\rangle$ varies slowly on the scale of the interaction length, the normalized growth rate is found to be

$$\bar{q}=\frac{\sqrt{3}}{2}\left[\frac{\alpha\Omega}{2\tau_0\beta_E}\left\langle\frac{1}{(\gamma_i\beta_i)^3}\right\rangle\right]^{1/3} . \tag{3.6}$$

Accordingly, the total gain is $g=20\log_{10}(\tfrac{1}{3}e^{\bar{q}})$.

B. Oscillator

For an ideal oscillator it is assumed that no variations in space occur and therefore the amplitude of the electric field affecting the electrons does not depend on the location of any individual electron. As a result we replace $a_+(\bar{z}_i(\tau),\tau)$ in the single-particle energy conservation [Eq. (2.18)] with its value at the input, $a_+(0,\tau)$, hence

$$\frac{d}{d\tau}\gamma_i(\tau)=-\beta_i(\tau)\tfrac{1}{2}[a_+(0,\tau)e^{j\chi_i(\tau)}+\text{c.c.}] . \quad (3.7)$$

The reflection coefficients from both ends are *unity*; in addition the boundary conditions imply $kd=\pi n$. As a result $R=1$ and the reflection condition [Eq. (2.23)] reads

$$a_+(0,\tau)=a_+(1,\tau-1/\beta_E) . \quad (3.8)$$

In order to determine the dynamics of the amplitude in an oscillator we average Eq. (2.25) over the interaction region:

$$\frac{d}{d\tau}a_+(0,\tau)+\beta_E[a_+(1,\tau)-a_+(0,\tau)] =\alpha\langle\beta_i(\tau)e^{-j\chi_i(\tau)}\rangle . \quad (3.9)$$

We now substitute the reflections' condition from Eq. (3.8):

$$\frac{d}{d\tau}a_+(0,\tau)+\beta_E[a_+(0,\tau+1/\beta_E)-a_+(0,\tau)] =\alpha\langle\beta_i(\tau)e^{-j\chi_i(\tau)}\rangle . \quad (3.10)$$

Expanding in a Taylor series with respect to $1/\beta_E$ we finally get

$$\frac{d}{d\tau}a_+(0,\tau)=\frac{\alpha}{2}\langle\beta_i(\tau)e^{-j\chi_i(\tau)}\rangle . \quad (3.11)$$

Equations (3.7) and (3.11) are the equations of an idealized oscillator. If we compare the equations which describe the dynamics of the amplitude of the radiation field in the case of the oscillator [Eq.(3.11)] with the corresponding one in an amplifier [Eq.(3.4)] we observe that there is a factor $\frac{1}{2}$ difference. This is due to the fact that in the oscillator, in the same volume, there are *two* waves to which the energy of the electrons is transferred. As in the case of the amplifier we now calculate the normalized growth rate. For this purpose we take the second derivative of Eq. (3.11); neglecting terms which oscillate at twice the frequency, to find the following expression for $a_+(0,\tau)$:

$$\left[\frac{d^3}{d\tau^3}+j\frac{\alpha K}{2}\left\langle\frac{\beta_i}{\gamma_i^3}\right\rangle\right]a_+(0,\tau) =-\frac{\alpha}{2}\langle\beta_i(\Omega-K\beta_i)^2e^{-j\chi_i}\rangle . \quad (3.12)$$

Assuming that $\langle\beta_i/\gamma_i^3\rangle$ does not vary significantly in time, the normalized growth rate is

$$\bar{\omega}=\frac{\sqrt{3}}{2}\left[\frac{\alpha K}{4}\left\langle\frac{\beta_i}{\gamma_i^3}\right\rangle\right]^{1/3} . \quad (3.13)$$

At this stage we do not wish to make any further comments on the idealized devices and we continue by determining the equations which describe the time-dependent interaction process in an amplifier.

IV. REFLECTIONS IN AN AMPLIFIER

There are two processes which may cause significant time variations in an amplifier: saturation and reflections. Saturation occurs when the initial amplitude of the radiation field is large or the interaction length is very long. An amplifier is generally designed to operate below the saturation level. However, if in the design process we disregard reflections then until the first reflection reaches the input the system will probably operate as designed. But as the first reflection adds to the initial amplitude the interaction may saturate. Variation in time caused by saturation without reflections involved is beyond the scope of this study.

At present we shall investigate the variation in time caused by reflections in an amplifier. The process is as follows: before the electron beam is injected in the structure the amplitude of the forward propagating wave is uniform in space and constant in time. Let us denote it by a_0. Ignoring the effects accompanied with the pulse front we may expect this amplitude to be amplified according to the equations determined previously. The change in this amplitude is propagating with the energy velocity $V_E\equiv c\beta_E$ so it will take approximately d/V_E for the amplified field to approach the output end and twice that time for the variation to arrive back to the input (we may define the bouncing period as $\tau_b\equiv 2d/V_E$). The ratio between the output and input amplitude of the forward propagating wave during the first bouncing period

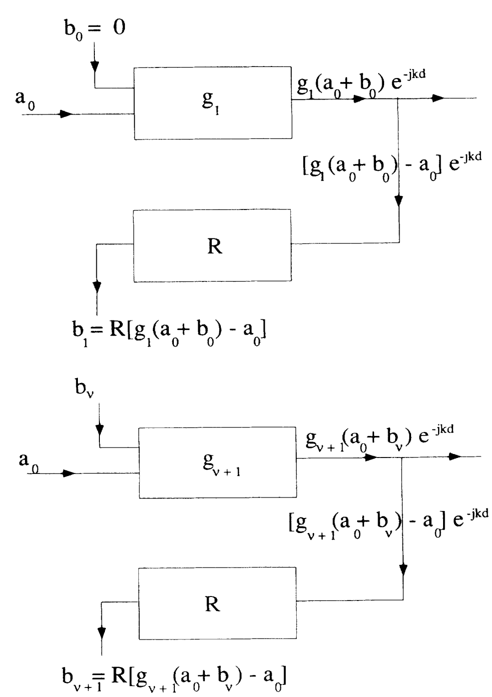

FIG. 1. Diagrammatic view of the reflection process.

is denoted by g_1 and it is referred to as the first one-pass gain. The reflections' contribution at the input will be denoted by b_ν, where ν is the index that numerates the bouncing process; therefore it can be considered as a discrete (normalized) time variable. During the first period the reflections have no contribution, therefore $b_0=0$. The amplitude at $\bar{z}=1$ is $g_1(a_0+b_0)e^{-jkd}$. Without the beam present the amplitude at this point is a_0e^{-jkd}. Therefore only the difference is reflected. After an additional reflection from the input end we may write the contribution of the first reflection to the amplitude at the input as

$$b_1=R[g_1(a_0+b_0)-a_0]\ . \tag{4.1}$$

Before this reflection arrives ($t<\tau_b$) the amplitude at the input is constant—its value being a_0. Until the next reflection arrives the amplitude at the input has two contributions which are constant in time. One from the generator and the other from the reflection, i.e., a_0+b_1.

After the νth reflection the amplitude at the input is a_0+b_ν and at the output end $g_{\nu+1}(a_0+b_\nu)e^{-jkd}$; the one-pass gain is therefore defined as the ratio between the output and input amplitude of the forward propagating wave during the same bouncing period. As a result, the contribution of the reflections to the input amplitude after $\nu+1$ steps is

$$b_{\nu+1}=R[g_{\nu+1}(a_0+b_\nu)-a_0]\ . \tag{4.2}$$

This process is summarized in Fig. 1. At the limit of a very long pulse, with linear gain such that $g_\nu=g$ for any ν, we have for $b_\nu=a_0R(g-1)/(1-Rg)$. This implies the amplitude at the input reads

$$a_0+b_\nu=a_0\frac{1-R}{1-Rg}\ , \tag{4.3}$$

exactly as predicted by a linear (steady-state) theory. Furthermore in Ref. [11] it was shown that the denominator is responsible for the result we mentioned in the Introduction, namely, that the *gain times bandwidth* product is constant in an amplifier.

Let us now consider a simple system within the framework of the present analysis. For this purpose we choose a dielectric-loaded waveguide with the wave number k given by

$$k=\left[\epsilon\frac{\omega^2}{c^2}-\frac{p_1^2}{R_0^2}\right]^{1/2}\ , \tag{4.4}$$

where R_0 is the radius and $p_1=2.4048\ldots$ is the first zero

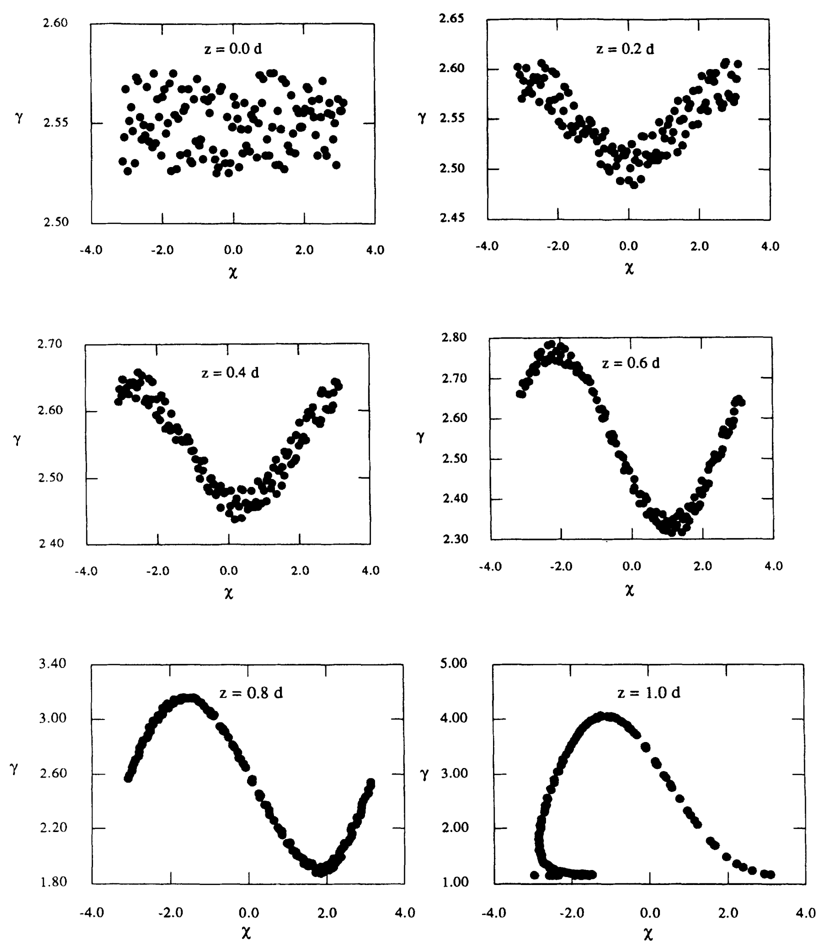

FIG. 2. Phase-space distribution at various locations along an ideal amplifier.

of the zero-order Bessel function. The other two parameters of our theory, α and β_E, are easily evaluated in this case and for a beam moving on the axis are given by

$$\alpha=\frac{eI(\mu_0/\epsilon_0)^{1/2}}{mc^2}\frac{1}{\{\epsilon[(\omega/c)R_0]J_1(p_1)/p_1\}^2}\frac{d^2}{\pi R_0^2}\frac{1}{\langle\beta\rangle_0}\ , \tag{4.5}$$

and

$$\beta_E=\frac{1}{\epsilon\beta_{\rm ph}}\ , \tag{4.6}$$

where the normalized phase velocity is defined as $\beta_{\rm ph}\equiv\omega/(kc)$ and we can readily see that if the dielectric coefficient ϵ is not frequency dependent then the energy velocity equals the group velocity.

We consider next the operation of an ideal amplifier for $\omega/2\pi=8.8$ GHz, $R_0=1.1$ cm, $d=20$ cm, $\epsilon=2.6$, $I=1$ kA, $\langle\gamma\rangle_{\rm input}=2.55$, and an input power of 80 kW. Figure 2 shows the phase-space distribution at different points along the amplifier. Starting from a uniform distribution at $\bar{z}=0$ we observe that at $\bar{z}=0.2$ the electrons which were in phase with the wave have been decelerated whereas these in antiphase were accelerated. A similar picture occurs at $\bar{z}=0.4$, however, here we observe that in addition to the further increase in the energy spread, there starts a shift in the location of the bottom point of the distribution. The amplification process starts at this point—see Fig. 3. As the electrons advance along the amplifier both processes continue ($\bar{z}=0.6,0.8$) until the decelerated electrons arrive at the point where they are in antiphase with the wave and they start being accelerated. Here saturation occurs—as indicated by the phase distribution at $\bar{z}=1.0$ and also by examining more closely the gain curve in Fig. 3. This simulation predicts a 32-dB gain in good agreement with the Pierce gain (34 dB) in spite the fact that the energy spread is not small (see Fig. 3) as assumed by the latter theory (for further discussion see Ref. [14]).

Our next step is to examine the variation in time of the gain due to the reflection process. Without loss of generality we choose both the reflection coefficients to be equal, $\rho_{\rm in}=\rho_{\rm out}=\rho$. The electron pulse is 100 ns long. In Fig. 4 we can see how the one-pass gain (squares) and the total gain (circles) are varying in time; ν indicates the index of the reflection, i.e., $\nu=1$ is reflection number one, etc. The total gain is the ratio between the accumulated amplitude, of the forward propagating wave, at the output and the initial amplitude (before the electron beam was injected) at the input of the interaction region. For small reflection coefficient, $\rho=0.1$, we observe that both gains are relatively stable. The fact that the total gain is smaller than the one-pass gain is not of particular significance at this point since this depends on the phase accumulated by the wave in its round trip as can be seen from the denominator in Eq. (4.3). However, as the reflections are increased the input amplitude increases, saturation is reached and therefore the one-pass gain is systematically smaller than the total gain. There exists an intermediary point, $\rho=0.5$, where the system acts very unstably whereas at another $\rho=0.7$ the system appears to be very stable in spite of the fact that the reflection is higher. This is a direct result of the phase dependence of the reflected amplitude. Ultimately at high reflection ($\rho=0.9$) the system reveals an immediate increase of the amplitude in time associated with practically zero one-pass gain, indicating that the system is operating as an oscillator. Notice that whatever the reflection coefficient was, before the first reflection arrives, the one-pass gain and the total gain are equal.

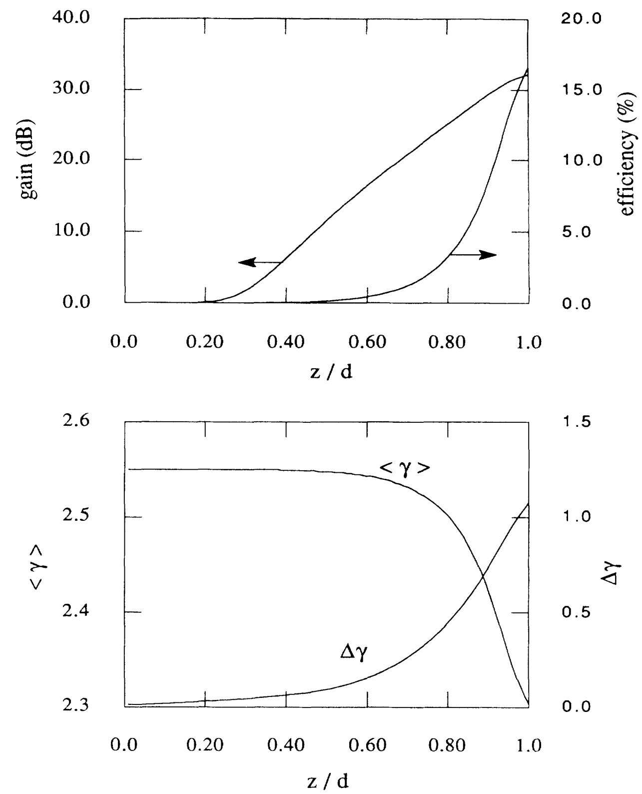

FIG. 3. The variation in space of the gain and efficiency (upper) corresponding to the same phase distribution presented in Fig. 2. The average energy of the electrons and their spread (lower) is also illustrated.

In order to show the general influence of the reflection coefficient on the total gain and the one-pass gain we have averaged out these two quantities over the entire number of reflections for different values of the reflection coefficient. The result is illustrated in Fig. 5. We observe here that the average one-pass gain monotonically decreases as the reflection coefficient increases. The average total gain is stable for small ρ corresponding to a linear regime of operation; it slightly decreases for intermediary reflections—corresponding to saturation—and it increases again when the reflection is so high that the system practically operates as an oscillator. Notice that in this case the one-pass gain is practically zero.

An additional insight of the physical process can be achieved by examining the spectrum of the signal as illustrated in Figs. 6 and 7. The power in each frequency component of the signal is normalized to the power in the central frequency (8.8 GHz). When the reflection is low ($\rho<0.15$) the power in all the other frequencies is 30 dB below the level of the main signal. For $\rho=0.2$ the eigen-

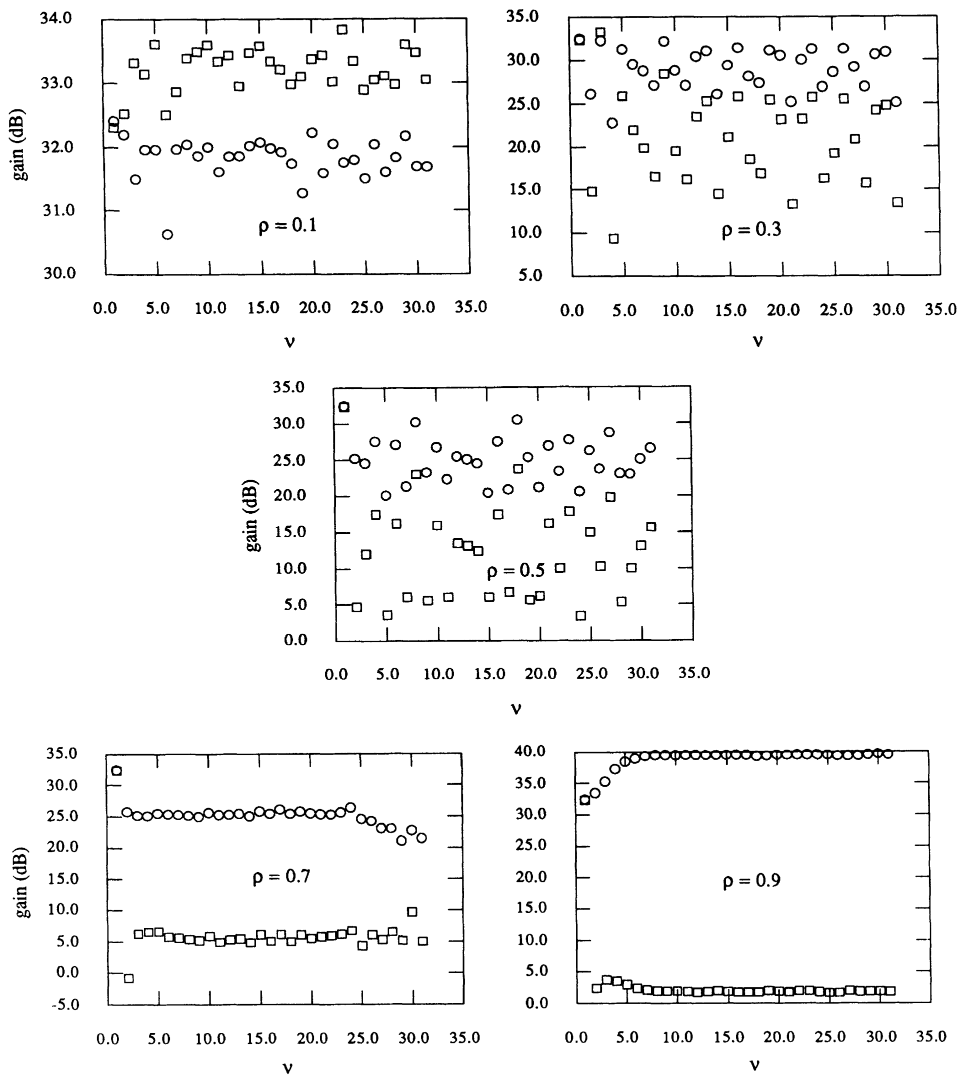

FIG. 4. The one-pass gain (squares) and the total gain (circles) for various reflection coefficients. Notice how for $\rho=0.9$ the one-pass gain drops to zero and the total gain grows in time indicating the system oscillates.

frequencies of the "oscillator" are less than 15 dB below the central frequency. The power in the sidebands is increasing monotonically with the reflection coefficient ρ, and at $\rho=0.4$ they dominate. These plots which correspond to a theoretical calculation can be compared, in Fig. 8, with fast-Fourier-transform (FFT) pictures of an amplified signal as reproduced from experimental data [8,9,13,15]. The bandwidth of the cold pulse is of order of 1 MHz. It is difficult to make a quantitative comparison since we do not know the reflection coefficient at both ends but the similarity in the general behavior of the experimental and theoretical results is apparent.

V. SPACE VARIATION IN AN OSCILLATOR

Part of the energy in an oscillator is extracted by making the reflection coefficient of the mirror(s) smaller than unity. As a result, the amount of electromagnetic energy available for interaction with the electrons decreases. Since this power is extracted at the ends, it is revealed as an effective variation of the field amplitude. In order to illustrate the effect of the spatial variation on the operation of an oscillator we start by integrating the equation which describes the dynamic of the amplitude [Eqs. (2.19) and (2.24)] over the entire length of the oscillator:

$$\frac{d}{d\tau}|a_+(1,\tau)|^2+\beta_E[|a_+(1,\tau)|^2-|a_+(0,\tau)|^2] =\alpha[a_+(1,\tau)\langle\beta_i(\tau)e^{-j\chi_i(\tau)}\rangle+\text{c.c.}] \ . \qquad (5.1)$$

Here we have assumed that the amplitude is slowly varying in space so that we replaced its average value with the value at the output. Next we substitute the reflections' condition from Eq. (2.23)—rather than Eq. (3.8) in the case of the ideal oscillator. The result is

$$\frac{d}{d\tau}|a_+(1,\tau)|^2+\beta_E[|a_+(1,\tau)|^2-|a_0(1-R)+Ra_+(1,\tau-1/\beta_E)|^2]=\alpha[a_+(1,\tau)\langle\beta_i(\tau)e^{-j\chi_i(\tau)}\rangle+\text{c.c.}] \ . \qquad (5.2)$$

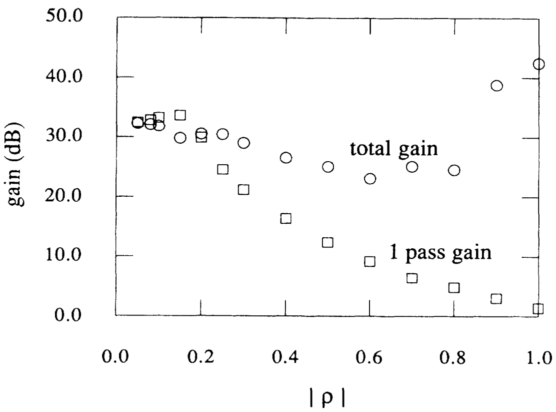

FIG. 5. The average one-pass gain and the average total gain for various reflection coefficients; the average is over all the reflections during the pulse. As the reflection coefficient increases, the one-pass gain decreases monotonically to zero. In parallel the total gain remains almost unchanged for small ρ. For intermediary values it decreases somewhat, indicating that saturation occurs. For higher ρ the system oscillates so that the total gain increases again.

Expanding in Taylor series with respect to $1/\beta_E$ and assuming $a_0=0$, we finally get

$$\left[\frac{d}{d\tau}+\beta_E\frac{1-|R|^2}{1+|R|^2}\right]a_+(1,\tau) = \frac{\alpha}{1+|R|^2}\langle\beta_i(\tau)e^{-j\chi_i(\tau)}\rangle \ . \qquad (5.3)$$

This expression replaces Eq. (3.11) in the description of a nonideal oscillator. The second term in the left-hand side of Eq. (5.3) represents the "radiation" loss due to the finite transmission from both ends of the oscillator.

The only source of energy in the oscillator is in the beam. When the mirrors are ideal, all the kinetic energy converted in radiation power is confined into the volume of the oscillator. If part of this energy is allowed to flow out, then self-sustained oscillation is possible only if the current injected is above a threshold value which depends on the reflection coefficients. In order to determine the threshold current we first have to notice that the radiation loss is associated with an exponential decay with a coefficient [see Eq. (5.3)] $\beta_E(1-|R|^2)/(1+|R|^2)$. For self-sustained oscillation this decay has to be smaller than the exponential increase due to the interaction—as determined in Eq. (3.13), i.e.,

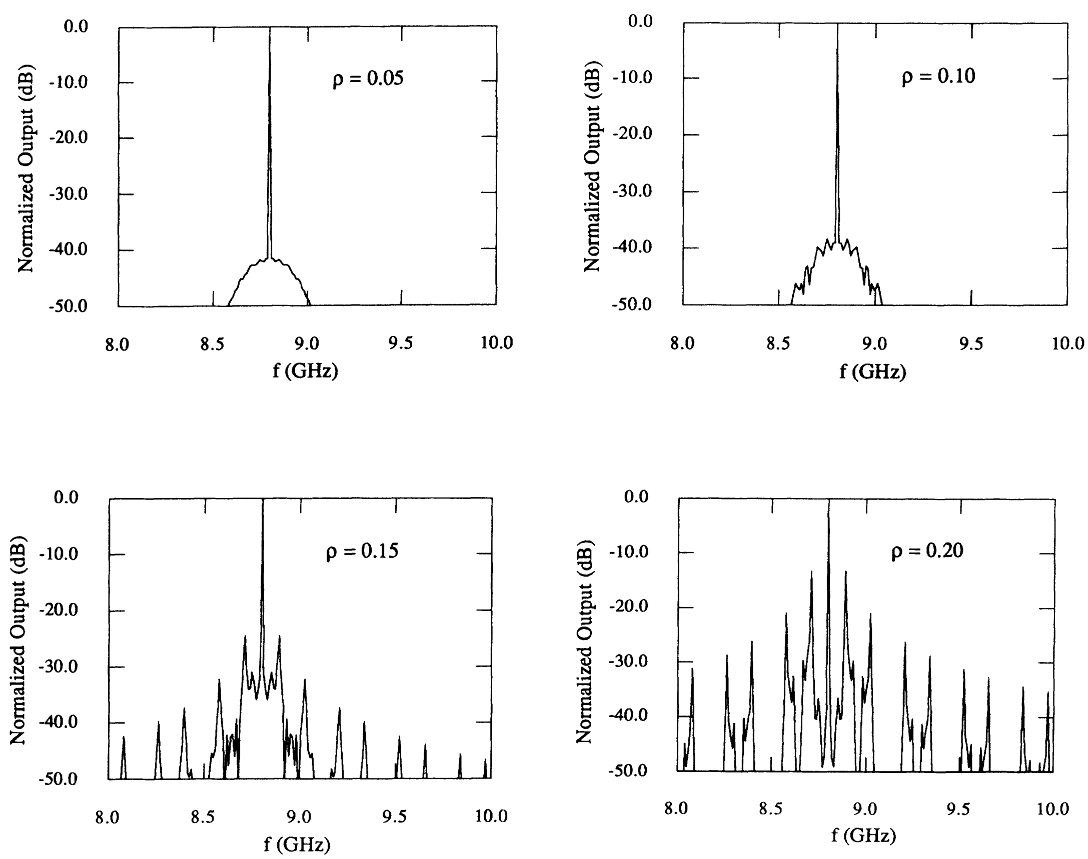

FIG. 6. The spectrum of the output signal for various reflection coefficients $(0.05<\rho<0.2)$, normalized to the output signal component at the input frequency.

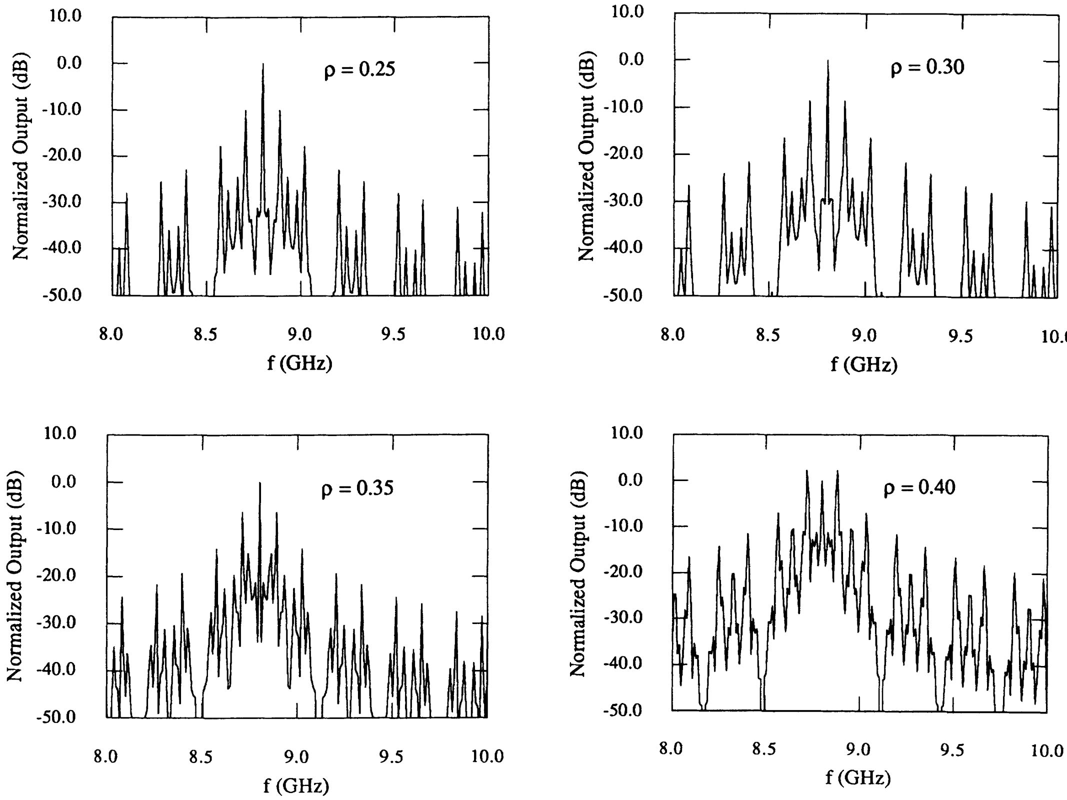

FIG. 7. The spectrum of the output signal for various reflection coefficients $(0.25<\rho<0.4)$, normalized to the output signal component at the input frequency.

$$\beta_E \frac{1-|R|^2}{1+|R|^2} < \bar{\omega} \equiv \frac{\sqrt{3}}{2}\left[\frac{\alpha K}{4}\left\langle\frac{\beta_i}{\gamma_i^3}\right\rangle\right]^{1/3} . \tag{5.4}$$

Therefore the condition for self-sustained oscillation can be formulated as

$$I > I_{\text{th}} \equiv \frac{mc^2/e}{(\mu_0/\epsilon_0)^{1/2}} \frac{4}{K\langle\beta_i/\gamma_i^3\rangle\langle\beta_i\rangle} \times \epsilon_{\text{eff}} \frac{s}{d^2}\left[\frac{2}{\sqrt{3}}\beta_E \frac{1-|R|^2}{1+|R|^2}\right]^3 . \tag{5.5}$$

The energy extracted from both ends is one mechanism responsible for spatial variations but it is not the only one. The electrons entering the oscillator are unbunched. The buildup of the bunches is not "immediate" in space but will take some portion of the interaction length. After this transient region there will be no variations in space, provided that the system does not reach saturation—which will not be considered here. In order to illustrate this effect, we examine the same system as in the case of the amplifier; in this case, however, the input power P_{in} is zero, the pulse length is 50 ns instead of 100 ns in the amplifier, and the "mirrors" at both ends of have a reflection coefficient $\rho=0.9$. The entire pulse was assumed to consist of 35 000 macroparticles, 512 of those being at any time in the oscillator. In Fig. 9 we illustrate the phase space of these electrons which are in the interaction region. In the first 20% of the pulse duration there is not sufficient electromagnetic energy built up in the oscillator to affect significantly the electron distribution (though if one compares, there is a small increase in the momentum spread). After 40% of the pulse has passed we clearly see the spatial transient. At this point in time the constant-amplitude regime is achieved after about 20% of the length of the oscillator. The normalized momentum spread which at the beginning is less than 0.06 is now larger than 0.35. Later in time the bunches continue to grow—the momentum spread is further increased approaching 3 at the end of the electrons' pulse. Although this spread is increasing, the spatial transient is confined to the first 40% of the interaction length and beyond this point the system acts as an ideal oscillator. This is revealed in the upper frame of Fig. 10 where the gain reveals a clear exponential increase in time. The gain in this case is defined as the total electromagnetic energy produced divided by the average kinetic energy of the beam. Prior to this exponential regime there is a transient which is similar to the transient revealed by Fig. 3, the difference in the behavior being due to the fact that in this case the initial field is zero. It is interesting to notice that this gain is larger as the reflection coefficient, ρ is smaller. This is at the expense of the bandwidth which is decreasing with ρ. Like the gain, the momentum spread is larger for smaller ρ—see the lower frame in Fig. 10.

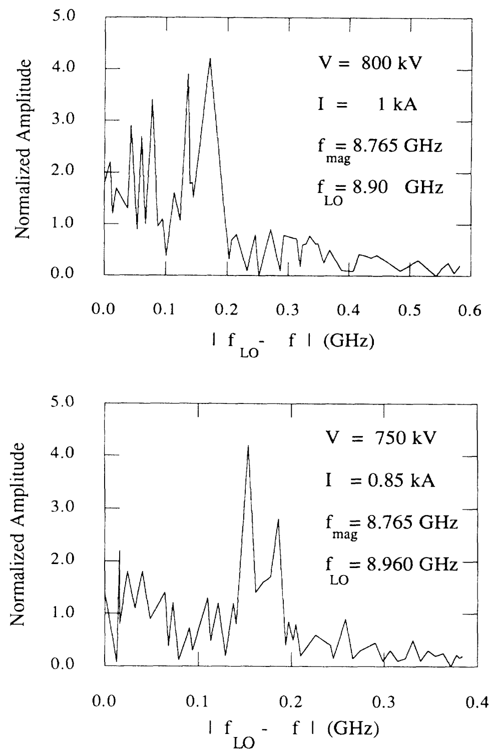

FIG. 8. The normalized spectrum of the output signal from two experimental shots. Notice the radiation adjacent peaks; the Magnetron is tuned in both cases to 8.765 GHz and its bandwidth is 1 MHz. f_{LO} is the lock-in oscillator frequency.

Before we conclude this section we wish to emphasize the difference between the two transients which occur in an oscillator. It is well known that the interaction in a traveling-wave tube within the fluid and linear approximations can be described as a superposition of three "eigenmodes" with decaying, constant, and growing amplitudes. If an initial field is present, then these steady-state solutions reveal that before the total field will start to grow exponentially there will be a transient period during which all three modes are equally participating and the amplitude of the field is practically unchanged. This effect is called lethargy, and is clearly revealed by Fig. 3 for an amplifier and may be found in Ref. [19] for an oscillator. However, the transient presented in Fig. 9 is different. It is not a result of the three eigenmodes mentioned above since in an "ideal" oscillator these modes have a constant amplitude in space. As we mentioned above this is a result of the finite length it takes the radiation field to bunch the "fresh" electrons.

A nonuniform bunching of the electrons in the interaction region implies that the amplitude of the forward propagating electromagnetic wave is expected to vary in space. The variation of the two distributions in space affects the efficiency of the interaction. The latter is expected to reach maximum when the two spatial distributions, of the radiation and of the electrons, are at maximum overlap. In very-short-pulse (picoseconds) free-electron lasers [20], the two distributions tend to separate, which is destructive to the interaction process.

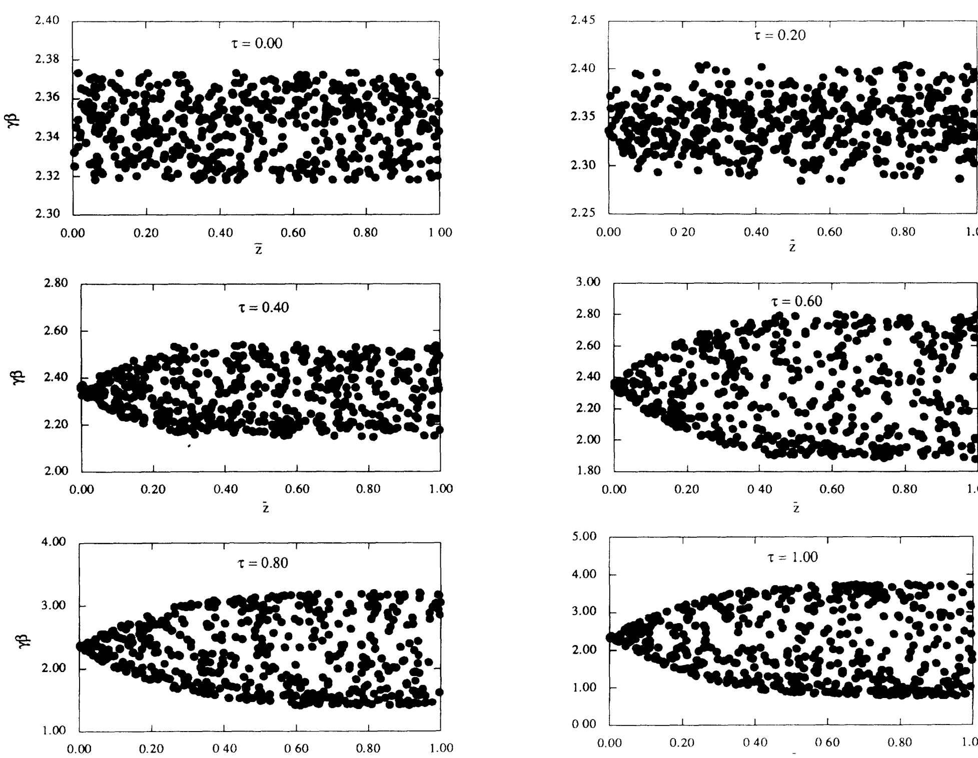

FIG. 9. The phase-space distribution in an oscillator at various times during the pulse duration. τ in this case is the time normalized to the total length of the electrons' pulse.

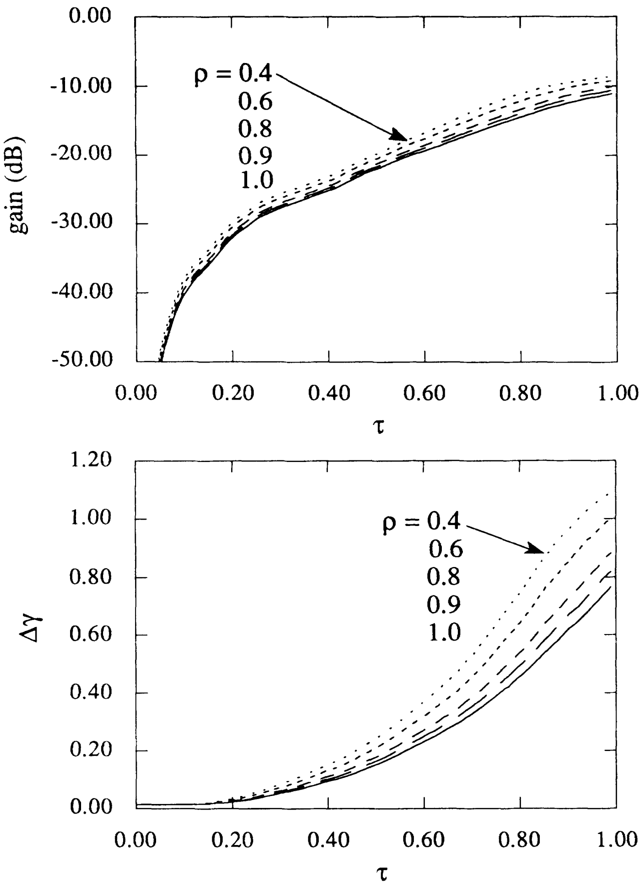

FIG. 10. The gain (upper) and the energy spread (lower) at various times during the pulse duration. τ in this case is the time normalized to the total length of the electrons' pulse.

For long-pulse (tens of nanoseconds) devices, which the present study addresses, this effect is probably less severe. A quantitative description of this effect requires a self-consistent solution of the governing equations, Eqs. (2.18), (2.23), and (2.25), which is beyond the scope of this study.

VI. CONCLUSIONS

We have shown that the convenient picture of a traveling-wave tube operating either as an amplifier or as an oscillator is too simplistic. In fact we have shown that these two regimes are the extreme cases and any system operates somewhere in between, corresponding to the reflection coefficients at both ends, the phase accumulated in one round-trip, and the gain. The interaction of a beam of electrons with an electromagnetic wave in a traveling-wave tube has been formulated so that it includes the effect of reflections.

In absence of reflections and saturation, in an amplifier, it is justified to assume that the electromagnetic wave amplitude remains constant in time. However, even very low reflection coefficients may affect the performance of an amplifier if the gain is very high. When reflections have been included in the analysis, the amplitude was shown to vary in time. The resulting spectrum was analyzed and the result reveals reasonable similarity with experimental data.

In an oscillator we have identified two major processes which cause spatial variations. The first is well known, namely, the process by which radiation power is extracted from the oscillator (a similar effect occurs with the Ohmic losses; this effect is ignored here). The second process revealed here is related to the fact that it takes some length until the new electrons, entering the oscillator, become bunched. As a result only in a part of the interaction region has the beam reached spatial "steady state" and therefore the effective length of the interaction is shorter than the geometrical length.

ACKNOWLEDGMENTS

This work was supported by AFOSR and DOE.

[1] Y. Carmel, J. D. Ivers, R. Kribel, and J. A. Nation, Phys. Rev. Lett. **33**, 1278 (1974).

[2] J. E. Walsh, T. C. Marshall, and S. P. Schlesinger, Phys. Fluids **20**, 709 (1977).

[3] S. P. Bugaev, V. I. Kanavets, A. I. Klimov, V. I. Koshelev, G. A. Mesyats, and V. A. Cherepenin (unpublished).

[4] J. E. Walsh, B. Johnson, G. Dattoli, and A. Renieri, Phys. Rev. Lett. **53**, 779 (1984); J. E. Walsh, in *Novel Sources of Coherent Radiation,* Physics of Quantum Electronics, edited by S. F. Jacobs (Addison-Wesley, Reading, MA, 1978), Vol. 5, p. 357.

[5] R. A. Kehs, A. Bromborsky, B. G. Ruth, S. E. Graybill, W. W. Destler, Y. Carmel, and M. C. Wang, IEEE Trans. Plasma Sci. **PS-13**, 559 (1985).

[6] E. P. Garate, R. Cook, P. Heim, R. Layman, and J. E. Walsh, J. Appl. Phys. **58**, 627 (1985), E. P. Garate, C. H. Shaughnessy, and J. E. Walsh, IEEE J. Quantum Electron. **QE-23**, 1627 (1987).

[7] K. Minami, W. R. Lou, W. W. Destler, R. A. Kehs, V. L. Granatstein, and Y. Carmel, Appl. Phys. Lett. **53**, 559 (1988).

[8] D. Shiffler, J. A. Nation, and C. B. Wharton, Appl. Phys. Lett. **54**, 674 (1989).

[9] D. Shiffler, J. A. Nation, and G. Kerslick, IEEE Trans. Plasma Sci. **PS-18**, 546 (1990).

[10] J. M. Butler, C. B. Wharton, and S. Furukawa, IEEE Trans. Plasma Sci. **PS-18**, 490 (1990).

[11] H. P. Freund and A. K. Ganguly, Phys. Fluids B **2**, 2506 (1990).

[12] L. Schächter, J. A. Nation, and G. Kerslick, J. Appl. Phys. **68**, 5874 (1990).

[13] D. Shiffler, J. A. Nation, J. D. Ivers, G. Kerslick, and L. Schächter, Appl. Phys. Lett. **58**, 899 (1991).

[14] L. Schächter, Phys. Rev. A **43**, 3785 (1991).

[15] D. Shiffler, J. A. Nation, J. D. Ivers, G. Kerslick, and L. Schächter, J. Appl. Phys. **70**, 106 (1991).

[16] L. Schächter, J. A. Nation, and D. A. Shiffler, J. Appl. Phys. **70**, 114 (1991).

[17] L. Schächter and J. A. Nation, J. Appl. Phys. **70**, 5186 (1991).

[18] Throughout this paper the reflection process is represented by a scalar coefficient, ignoring the effect of the evanescent waves present near both ends.

[19] R. Bonifacio, C. Pellegrini, and L. M. Narducci, Opt. Commun. **50**, 373 (1984).

[20] See H. Al-Abawi, F. A. Hopf, G. T. Moore, and M. O. Scully, Opt. Commun. **30**, 235 (1979), and also Refs. 9–12 therein.